A KD-trees based method for fast radiation source representation for virtual reality dosimetry applications in nuclear safeguards and security

Teófilo Moltó Caracena[a], Eduardo Vendrell Vidal[a], João G.M. Gonçalves[b], Paolo Peerani[b]

[a] *Universitat Politècnica de València, Camino de Vera s/n, Valencia 46022, Spain;*

[b] *Joint Research Centre, European Commission, Via E. Fermi 2749, 21027 Ispra VA, Italy*

Abstract:

With the aim of demonstrating the concrete advantages that novel technologies such as Virtual Reality (VR) can provide to the nuclear industry, the authors of this paper have been working on the development of a VR based simulator of a gamma dose rate detector for training purposes, to be applied in the field of nuclear security and safety.

Historically in nuclear science, simulating gamma dose rate transport has had a series of requirements, most importantly the accuracy of the computation. When embedding this dose rate computation in the environment of a VR based application, a second and opposing key requirement appears: real time performance. Meeting this requirement is only possible if a fast method to compute gamma radiation is used.

In order to achieve this target the authors have been working in ways of improving the efficiency of the Point-Kernel method by reducing its computational effort. This paper presents the latest step in this pursuit of efficiency; a novel method based on a non-regular kernel approach, combined with a KD-tree based volume division method. Devised to reduce as much as possible the number of points that represent the volume of the source while aiming at retaining sufficient dose computation accuracy.

Keywords: *simulation; dose rate; gamma radiation; training; point kernel;*

1. Introduction

Although there is not an official definition of what Virtual reality is, academia [1] has since its inception, described it as a wide concept which involves the combination of both hardware and software elements that make possible simulation of three dimensional environments which manage to transmit a sense of realism to the user. This paper focuses on the software side of VR, presenting an algorithm which prioritizes speed above other requirements, which is a distinguishing characteristic of VR software.

VR technologies have proven to be a successful tool for training activities in many fields of research and industry. In the specific areas of Nuclear Safeguards and Security, the first works started to appear in the 1990s [2-3] and nowadays several applications have demonstrated the potential of this technology to complement and enhance the traditional training methods [4-8]. VR technologies represent advantages in terms of cost reduction, safety and time scheduling. Nevertheless the use of VR requires software solutions that are capable of meeting the real-time constraints imposed by this technology.

To tackle the real-time issue, it is necessary to use the Point-Kernel (PK) [9] method as the fastest technique for dosimetry computation. Other methods like Monte Carlo [10] or Discrete Ordinates (S_N) [11] are discarded, because albeit more accurate, they are computationally more intense and therefore slower, as agreed by the scientific community [12-14].

Given the fact that the computational cost of a PK method is proportional to the number of points which make the point mesh of the nuclear source, the objective of a VR oriented PK method is to reduce the number of points in the mesh. The authors' research has focused on ways to achieve this, while affecting accuracy as less as possible.

2. Development of the method

2.1. VR Application

A possible scenario for a VR application in nuclear safeguards and security is the training of first response personnel (customs agents, law enforcement, fire and rescue service etc.) With this aim, the JRC developed some prototype VR applications so the trainee is immersed in a realistic scenario, where he or she needs to perform a specific task. The following images show two scenarios used in these VR prototypes.

Figure 1 VR training scenarios: spent nuclear fuel storage site (left) and customs inspection area (right)

Within these scenarios, the trainee needs to use a portable dosimeter to detect and identify radiation sources. Therefore, realistic 3D models of the detectors such as the one shown in the following figure where included in the application for the trainees to learn their use, interface details etc.

Figure 2 Real detector (left), simulated detector in VR application (right)

For the application to be truly useful from a training point of view, not only detailed imagery was required but also a realistic dose rate feedback to be shown on the VR detector interface. To meet this demand, algorithms to perform dose rate computations fast enough to work in the VR environment were required. This is the motivation for the algorithm presented in this paper.

2.2. Background

The first version of the dosimeter simulator implemented a simple mono-PK method [5], i.e. all nuclear sources where represented by a single point in space without volume. This solution although being extremely fast was lacking the required dose rate computation accuracy in certain conditions (short distances and large sources) and therefore it was not an acceptable solution.

This problem is solved in most other PK codes by representing the whole volume with a mesh of regularly spaced points [15]. This approach is adequate for the purpose that these software tools are made for: shielding design computations. In the case of VR applications, the real time requirement restricts this solution to very low density meshes, because increasing the point density increases the computational effort exponentially, making it too slow for these kind of applications.

To deal with this problem a second version was developed [16], featuring a non-regular division of the source volume which tries to exploit the fact that not all the volume of the source is equally significant in terms of dose rate. Therefore, closest regions of the volume are given a higher point resolution, leading to a non-regular division of the volume.

When increasing the resolution of an area is not a straightforward issue, the proposed method

3

uses the solid angle of the source with respect to the detector's point of view as a global parameter that takes into account distance, size and orientation of the source.

This method yielded a good result in comparison with the fixed-point mesh methods, achieving an acceptable accuracy while reducing significantly the number of points.

Nevertheless this method was based on the oct-tree generated division [17], which creates a minimum of eight points per each division step. This increase in points might not be completely necessary, given the accuracy requirements established. Therefore, this paper explores the use of a lighter division strategy, substituting the use of the oct-tree based division with the KD-tree division method.

The following figure illustrates the reduction in number of mesh points generated between the different division strategies previously explained after two division iterations.
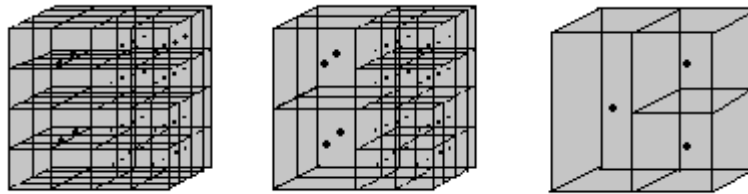

Figure 3: Oct-tree regular division (left), Oct-tree non-regular division (center), KD-tree division (right)

2.3. Point kernel method used

The point kernel method used computes the equivalent dose rate $D^{eq}(d)$ as described by the following expression, where (C) represents a conversion constant which accounts for this fluence-to-dose conversion, (A) the activity of each source point (j), (E$_i$) the energy and (P$_i$) the yield for each energy line (i). The build-up factor is represented by (B) while the attenuation is represented by $e^{-\mu_i t}$ where (μ) is the attenuation coefficient and (t) the thickness of the material. Also the energy absorption coefficient (μ/ρ) is taken into account. The (d) represents the distance between the source point and the detector point in the system of coordinates of the virtual environment, the rest of parameters are obtained via linear interpolation of data tables [18] . Finally the outer summation loop from one to 'm', stands for the number of sub-sources that represent the whole volume.

Equation 1

$$D^{eq}(d) = \sum_{j=1}^{j=m} \frac{C\ A_j\ \sum_{i=1}^{i=n} B_i E_i\ P_i\ e^{-(\mu_i\ t_j)_{shield}} \left(\frac{\mu}{\rho}\right)_i^{air}}{4\pi d_j^{\ 2}}$$

2.4. KD-trees

K-Dimensional trees (KD-trees) are a type of binary space partitioning tree [19], created with the aim of having a data structure which allows fast searching and sorting when handling ordered data. The way in which data is split can be applied to source volume representation.

In order to create the tree, a splitting rule is used to divide the space iteratively (in our case the

4

volume of the source). The space is split in two groups using a hyperplane orthogonal to the coordinate axes. This hyperplane cuts the space at a point determined by the splitting rule used.

Several splitting rules exist which try to optimize the speed of the algorithm in searches depending on the nature of the data that need to be sorted. The most spread and well-known method for partitioning KD-trees is the Standard split rule [18] (the following figure illustrates how this rule works). Other splitting rules have been created since, aiming at better performance in searches like [20] or [21] but all of these are designed for better dealing with clustered data points sets or other particular cases.

These situations are not related to our problem, where a single homogenous source is considered, implying mesh points are to be spaced uniformly, and therefore the adequate splitting method in this case is the original Midpoint split rule. This rule places the splitting hyperplane in the center of the axis of reference. The way this rule works is by first choosing the axis corresponding to the longest side of the volume. In case there are several equal length sides, the axis is chosen in a fixed cyclic manner (X-Y-Z), bisecting the volume as seen on the following figure.
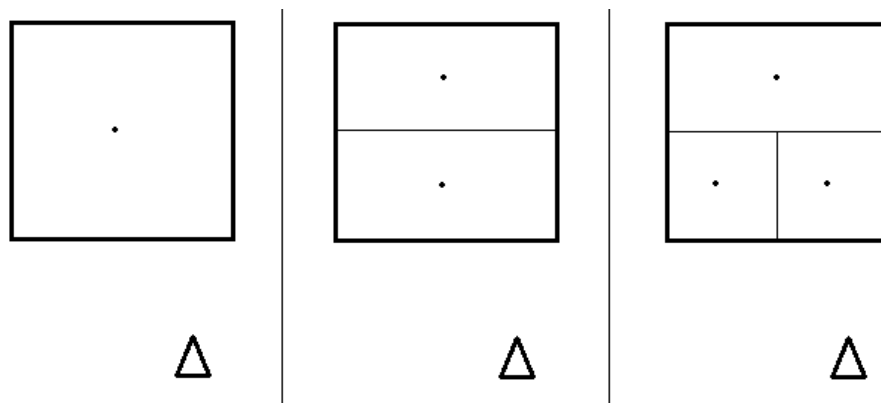

Figure 4: Midpoint splitting rule example. Initial state (left), first iteration (center), second iteration (right). The triangle represents the detector's position.

2.5. Comparison between KD-trees and Oct-trees

The Oct-tree method divides the volume by splitting in half each of its three axes in every iteration, unlike the KD-tree method which only tackles one axis at a time. In numerical terms, for each volume unit, the Oct-tree method generates eight units while the KD tree only generates two. To exhibit graphically the difference in behavior between the two methods, the example from the previous figure will be used. Starting with the same initial volume and detector position, two iterations of both methods are performed showing the results in the following figure.
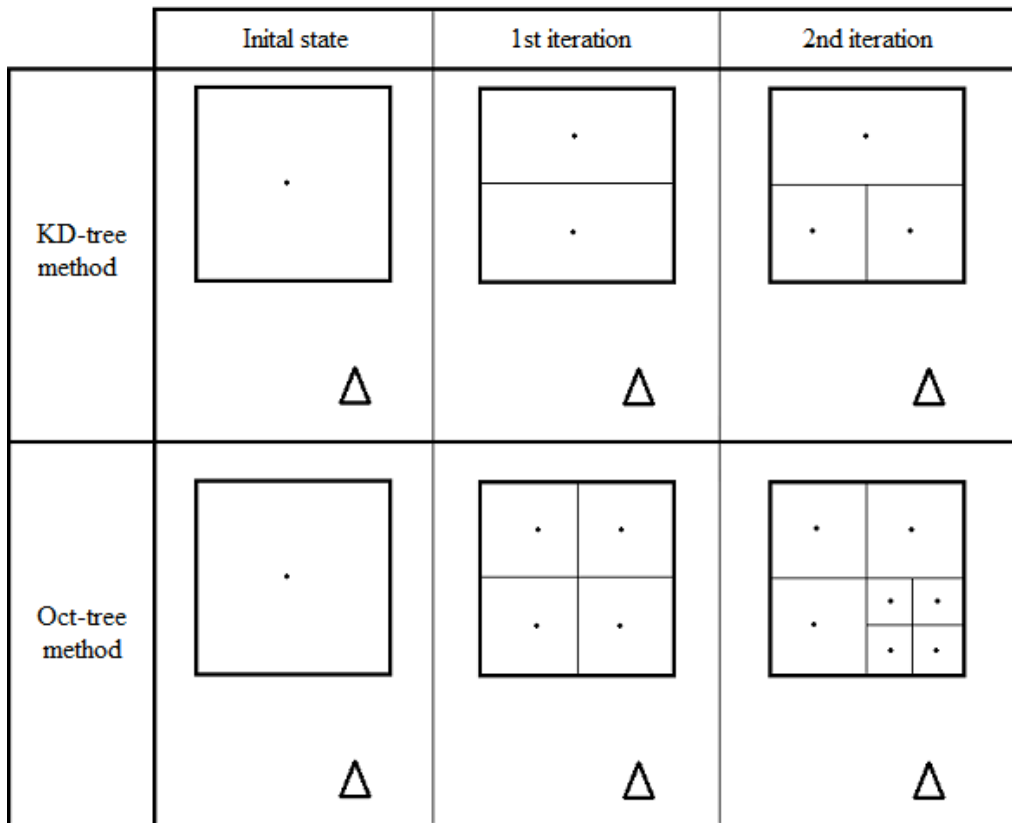
Figure 5 Two dimensional view of KD-tree vs Octree example

In the first iteration, the Oct-tree generates eight sub-sources compared to the KD tree's two. In the second iteration, the Oct-tree is using twenty-two sub-sources to represent the original volume compared to the three sub-sources the KD-tree method uses for that same case. A clear reduction in number of source points is apparent, hence the motivation to pursue the use of this new method.

2.6. Developed method based on the KD-tree concept

The KD-tree based volume division method uses a variant of the Midpoint split rule. This method acts as follows.

First, in order to produce coherent results, the division must take into account the starting position of the detector with respect to the source. Otherwise given the same distance, different results would be obtained depending on which side of the source the detector is. Therefore, a pre-computation based on the angle between the source direction and source-detector vector is done as shown on the following figure.
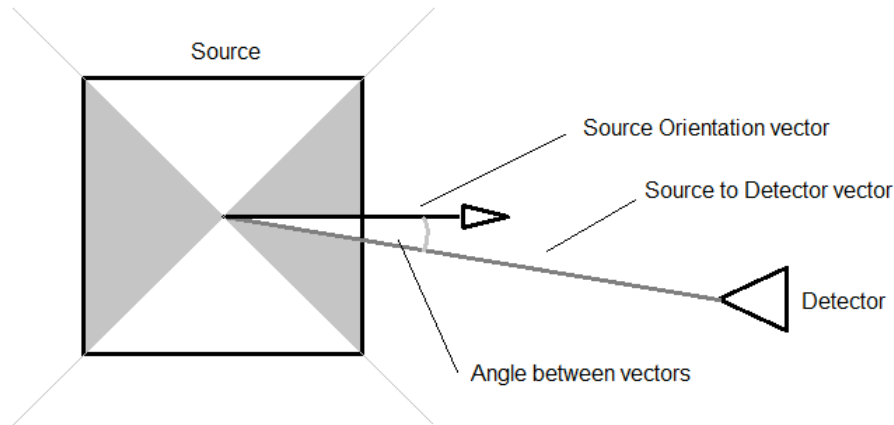
6

Figure 6: Starting axis choice (2D simplification). If the angle is within the areas marked in grey the first division is along the source orientation vector axis, otherwise the perpendicular axis is chosen.

Once the axis that will be split in first place has been chosen, this value is stored in the source definition. The devised splitting rule iteratively selects an axis to divide starting from the initially computed one, establishing a X-Y-Z cycle of divisions until no more steps are needed.

This KD-tree based division method only generates one sub-source per iteration, compared to the previously developed oct-tree based method that yielded eight sub-sources per each father source, therefore avoiding the creation of unnecessary sub-sources and keeping computational cost of running the multi-PK algorithm (which is proportional to the number of sub-sources) to a minimum.

3. Testing

Two sets of tests were carried out in order to evaluate the accuracy and performance of the software tool. First, a comparison with the dose rate obtained from a real detector with the aim to confirm that the accuracy error is tolerable for the purpose. Second, to quantify the computational cost gain obtained from the KD approach, its results are compared with respect to the previous version and with respect to the existing volume division methods [14].

The selected source is a stack of potassium chloride fertilizer sacks containing the 40K radioisotope. This source is a typical example of harmless source that can trigger the radiation portal's alarms at border crossings and therefore it is used often for training exercises. We are considering this as the only source contributing to the total dose.

The handheld detector used is a gamma ion chamber survey meter, model Victoreen 451P from Fluke industries. This device was chosen because it is commonly used in nuclear security activities and therefore it represents a valid tool for comparison.

The computer simulations were performed on a workstation equipped with a Intel E5640 2.67GHz processor, 3.49GB of RAM memory and a NVIDIA Quadro FX 3800 graphics card, using Virtools version 5.0 on Windows 7 Pro (32bit).
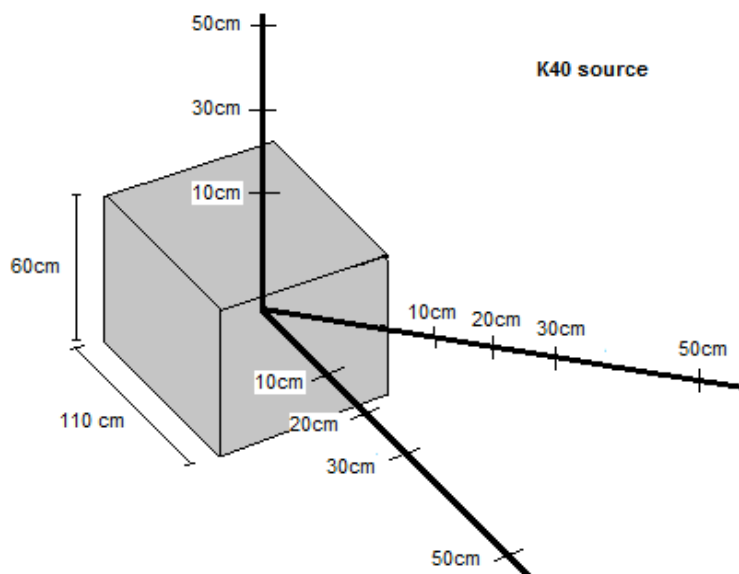
Figure 7: Set up of the experiment, measurement positions for the real detector and source.

The previous figure shows the experiment setup and a geometrical description of the source volume.

Measurements were taken with the hand-held detector on a series of points varying the distance to the source and the orientation from which the source is approached (front, diagonal, top). The purpose is to see how the new algorithm copes with distance and geometry changes.

4. Results

4.1. Dose rate accuracy of KD-tree simulation vs. real detector

The following table shows the readings taken with the real detector and the dose rate values computed with the new KD-tree based method in the simulator and the deviation of these with respect to the real measurement values.

Table 1. Real measurements vs. KD-tree simulation

Distance [cm]	Dose Rate received [μSv/h (Air)]		Deviation [%]
	Victoreen 451P	KD application	
Frontal			
50	0.09	0.10	10%
30	0.17	0.19	11%
20	0.23	0.26	13%
10	0.37	0.37	0%
Diagonal			
50	0.06	0.04	33%
30	0.1	0.08	20%
20	0.14	0.11	21%
10	0.19	0.17	11%
Top			
50	0.18	0.18	0%
30	0.25	0.28	12%
10	0.48	0.46	4%

The deviation of the dose rates obtained are all within tolerable limits (under 25% deviation) except for the furthest point in the diagonal case. The deviation of this result (33%) is over the established limit but it corresponds to such a low dose rate value (under 0.1 μSv/h) where the manufacturer of the survey meter does not guarantee any degree of accuracy.

### *4.2. Computational performance of KD-tree based method vs. previous methods.*

The following table resumes the execution time and number of points per mesh for all the tested cases considering three division methods: the new KD-tree based division method, the previous Oct-tree based division method and a standard regular division method with the point density equal to the highest point density areas in the Oct-tree VR method.

Table 2. Computational analysis of the different methods

Distance	KD division	Oct division	Regular division
[cm]	Time [ms] / Points	Time [ms] / Points	Time [ms] / Points
	Frontal		
50	20 / 6	25 / 8	25 / 8
30	53 / 18	105 / 36	190 / 64
20	76 / 26	191 / 64	1536 / 512
10	153 / 52	378 / 120	12288 / 4096
	Diagonal		
50	15 / 4	25 / 8	25 / 8
30	26 / 8	64 / 22	192 / 64
20	34 / 11	66 / 22	192 / 64
10	72 / 25	146 / 50	1536 / 512
	Top		
50	36 / 12	103 / 36	192/ 64
30	58 / 20	102 / 36	192 / 64
10	171 / 60	463 / 148	12288 / 4096

To clearly illustrate the trends in computational cost growth present in the previous tables, the data is shown in the following two figures in a graphical manner.

The line tagged "RT limit" denotes the maximum amount of time a computation can take before breaching the real-time constraint. In other words, methods whose results lie above this line are not valid for a VR task.
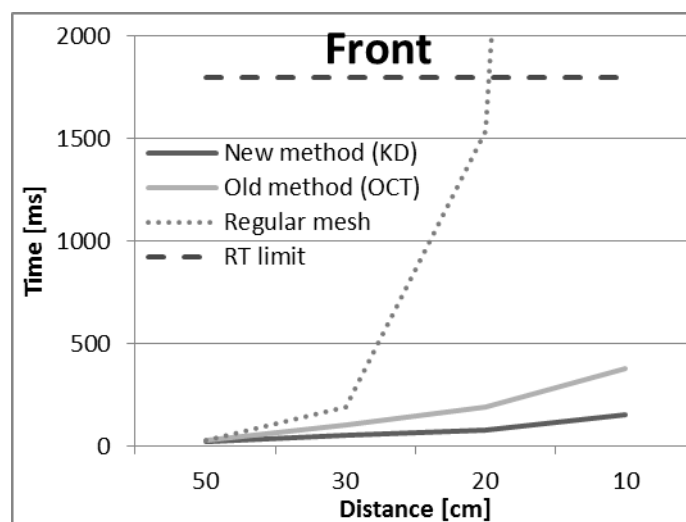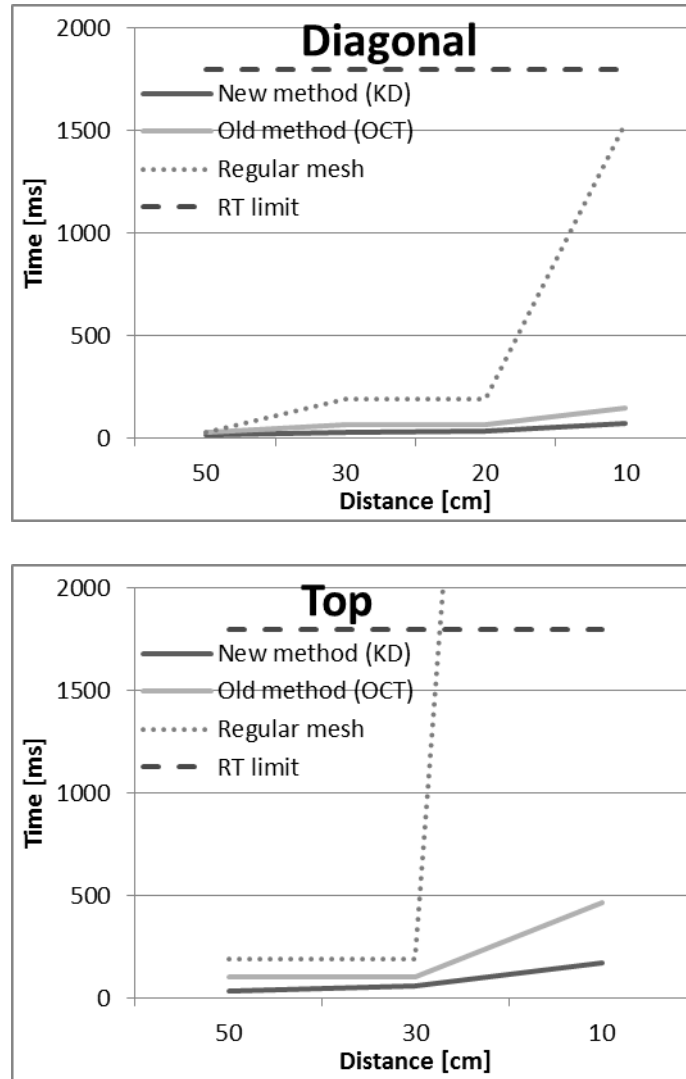
Figure 8: Computational analysis of the different method by orientation approach.

The results show that the regular mesh method violates the real time restriction in all three cases tested. On the contrary both the Oct-tree and the KD-tree based methods are valid solutions. The difference between these two is that the new KD tree method performs equally or better in all three cases for all instances tested.

5. Conclusion

When developing VR applications for dose rate computation (i.e., in nuclear handheld detector training purposes), modeling nuclear sources as a mesh of regularly spaced points is not feasible because a linear resolution increase (doubling the points per unit length) results in increasing computer effort exponentially and violates real time limitations after a few iterations in most cases.

This problem requires a solution that reduces the number of mesh points that need to be computed by the VR application. This paper shows how a KD tree based solution can be a valid method for such task, representing a faster solution than the existing oct-tree based

11

predecessor.

The KD-tree method reduces the computational effort (and therefore response time) by over 50% in comparison to the oct-tree based method, while retaining the necessary accuracy. Therefore, allowing the users to execute the application in slower devices, or to compute more sources in the same amount of time.

Acknowledgements

References

[1]   Brooks F.P, What's real about virtual reality? IEEE Computer graphics and applications, 1999; 19(6); 16-27.

[2]   Stansfield S. Application of Virtual Reality to Nuclear Safeguards and Nonproliferation. Albuquerque (USA): Sandia National Laboratories; 1996.

[3]   Vermeersch F, Van Bosstraeten C. Development of the VISIPLAN ALARA planning tool. Proc. Int. Conf. on Topical issues in Nuclear Radiation and Radioactive Waste Safety; 1998 Aug 31 – Sep 4; Vienna (Austria)

[4]   Moltó Caracena T, Brasset D, Vendrell Vidal E, Ruiz Morales E, Gonçalves JGM. A design and simulation tool for nuclear safeguards surveillance systems. ESARDA 31st annual meeting; 2009.

[5]   Moltó Caracena T, Gonçalves JGM, Peerani P, Vendrell Vidal E. Virtual reality based simulator for dose rate calculations in nuclear safeguards and security. ESARDA symposium; 2011; Budapest (Hungary).

[6]   Machado DM, Cotelli A, Galvão D, Mól AC, Carvalho PV, Vidal MCR. Use dosimetry virtual tool for security studies physics and nuclear. Procedia Manufacturing; 2015; 3, 1765-1771.

[7]   a Silva, MH, do Espírito Santo, AC, Marins, ER, de Siqueira, APL, Mol, DM, & de Abreu Mol, AC. Using virtual reality to support the physical security of nuclear facilities. Progress in Nuclear Energy; 2015; 78; 19-24.

[8]   Xi C, Wu H, Joher A, Kirsch L, Luo C. 3-D virtual reality for education, training and improved human performance in nuclear applications. Urbana. 2009 Apr 5; 51:61801.

[9]   Berger MJ, Improved point kernels for electron and beta ray dosimetry. Washington, DC: US Department of Commerce, National Bureau of Standards ;1973; NBSIR 73-107.

[10]   U. S. Metropolis N. The monte carlo method. Journal of the American statistical association; 1949; 44, 247 , 335-341.

[11]   Chandrasekhar S. Radiative transfer; Courier Dover Publications; 1960.

[12] Smith LE, et al. Coupling deterministic and Monte Carlo transport methods for the simulation of gamma-ray spectroscopy scenarios. IEEE Trans. Nucl. Sci. 2008 Oct; 55 5.

[13] Warren GA, Smith LE, Cooper M, Kaye W. Evaluation Framework for Search Instruments. IEEE Nucl. Sci. Symposium Conf. record; 2005

[14] Prokhorets IM, Prokhorets SI, Khazhmuradov MA, Rudychev EV, Fedorchenko DV. Point Kernel method for radiation fields simulation. Probl. Atom. Sci. Technol; 2007; 48, 106

[15] Vela O, De Burgos E, Perez JM. Dose rate assessment in complex geometries. IEEE Trans. Nucl. Sci. 2006 Feb; 53 1.

[16] Moltó Caracena T, Gonçalves JGM, Peerani P, Vendrell Vidal E. A variable point kernel dosimetry method for virtual reality simulation applications in nuclear safeguards and security. IEEE Transactions on Nucl. Sci. 2013; 60(5); 3862-3871.

[17] Jackins CL, Tanimoto SL. Oct-trees and their use in representing three-dimensional objects. Computer Graphics and Image Processing. 1980; 14(3); 249-270.

[18] Trubey D, Hubbell JH. Gamma-ray attenuation coefficients and buildup factors for engineering materials. American National Standard—ANS-6.4. 3. 1991.

[19] Bentley JL. Multidimensional binary search trees used for associative searching. Communications of the ACM. 1975; 18(9); 509-517.

[20] Friedman JJ, Bentley JL, Finkel RA. An algorithm for finding best matches in logarithmic expected time. ACM Trans. Mathematical Software. 1977 Sep; 3:209-226.

[21] Maneewongvatana S, Mount DM. It's okay to be skinny, if your friends are fat. 4th Annual CGC Workshop on Computational Geometry. 1999.